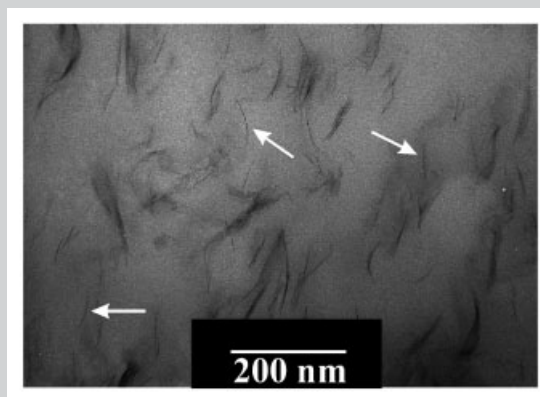


Summary: Both intercalated and exfoliated poly(L,L-lactide) (P(L,L-LA)/organomodified montmorillonite nanocomposites were synthesized by in situ ring-opening polymerization of L,L-lactide, in bulk, directly in the presence of the nanofiller. Intercalation of polyester chains was found to appear even for natural unmodified montmorillonite-Na⁺, while exfoliation occurred when the aluminosilicate layers were modified by ammonium cations bearing primary hydroxyl groups. Clay delamination was effectively triggered by the grafting reaction of the growing PLA chains onto the hydroxyl groups. Aluminium triisopropoxide, triethylaluminium, and stannous octoate, as initiating or co-initiating species, were compared in terms of polymerization control. The influence of nanoclay content (from 1 to 10 wt.-% in inorganics) on morphology and thermal behavior was also studied. In parallel, a highly filled nanocomposite (called masterbatch), prepared by in situ polymerization, was dispersed into a (plasticized) preformed polylactide matrix in the molten state, to reach a better clay delamination than that obtained by direct melt blending. Finally, L,L-lactide and α,ω -dihydroxylated poly(ethylene glycol) (PEG 1000) were copolymerized

in presence of clay in order to study the behavior of the resulting triblocks towards nanocomposite formation.



Significant exfoliation of clay platelets has been achieved in a commercial polylactide matrix using a “masterbatch” process (white arrows).

(Plasticized) Polylactide/(Organo-)Clay Nanocomposites by in situ Intercalative Polymerization

Marie-Amélie Paul,¹ Cécile Delcourt,¹ Michaël Alexandre,¹ Philippe Degée,¹ Fabien Monteverde,² André Rulmont,³ Philippe Dubois*¹

¹Laboratory of Polymeric and Composite Materials (LPCM), University of Mons-Hainaut, 20 place du Parc, 7000 Mons, Belgium
Fax: 00 32-65 37 34 84; E-mail: philippe.dubois@umh.ac.be

²Laboratory of Analytic and Inorganic Chemistry (LAIC), University of Mons-Hainaut, 20 place du Parc, 7000 Mons, Belgium

³General Chemistry and Physics Chemistry Department, University of Liège, Building B6, 4000 Liège, Belgium

Received: August 5, 2004; Revised: November 12, 2004; Accepted: December 21, 2004; DOI: 10.1002/macp.200400324

Keywords: nanocomposites; organoclay; poly(L,L-lactide); ring-opening polymerization

Introduction

During the last decade, the introduction of nanofillers in biodegradable matrices has allowed to improve the range of properties and possible uses of these environmental-friendly polymers. Amongst nanofillers, layered aluminosilicates such as montmorillonite, have been largely studied.^[1] Considering poly(L,L-lactide) (P(L,L-LA)) matrix, direct melt blending of the polyester with the clay leads to intercalated or, at best, semi-intercalated/semi-exfoliated nanocomposites, whatever the investigated clay surface cationic organomodifier,^[2] even with the use of a compatibilizer as poly(ϵ -

caprolactone) (PCL) or the presence of poly(ethylene glycol) (PEG) as plasticizer.^[3,4] Even if intercalation of polymer chains into the interlayer spacing of layered aluminosilicates brings noticeable improvement in term of mechanical, thermal, and barrier properties compared to unfilled matrix, complete delamination of the clay platelets by polymer chains has proved, for several kinds of polymer,^[5] to reinforce to a much larger extent the pre-cited properties.

One of the best methods known to achieve exfoliation consists in promoting the matrix polymerization from initiators located on the clay surface. Such a technique has been successfully applied to the preparation of polyamide

6,^[6] polyamide 12,^[7] poly(methyl methacrylate), and polystyrene based nanocomposites.^[8,9] This technique has been recently approached in case of ring-opening polymerization of lactones for the preparation of poly(ϵ -caprolactone)/layered aluminosilicate nanocomposites. Tin (II) octoate ($\text{Sn}(\text{Oct})_2$) and dibutyltin (IV) dimethoxide have been reported to efficiently promote the polymerization of ϵ -caprolactone in the presence of organomodified clays.^[10,11] The “grafting” of PCL chains onto montmorillonite, surface-modified by ammonium cations bearing hydroxyl groups, has also been studied. After activation by tin derivatives, the OH groups proved to be highly efficient for initiating the lactone polymerization and “grafting” the PCL chains onto the layered silicate surface. The density of surface hydroxyl functions has been tuned as a parameter controlling both the molecular weight of the polyester chains and the extent of clay exfoliation.^[12]

In a very recent communication,^[13] preliminary experiments on the synthesis of fully exfoliated P(L,L-LA)-based nanocomposites have been reported, as obtained by the in situ intercalative coordination-insertion polymerization of L,L-lactide promoted directly from the interlayer space of the organomodified montmorillonite. In line with this first communication, this paper aims at studying the effect of such a polyester chain grafting reaction on the nanocomposite morphology and thermal properties by comparing two different organomodified clays, bearing or not hydroxyl functions. In parallel, the influence of clay loading on the morphology, the thermal properties, and the crystallization behavior has been studied as well.

In a second approach, in situ polymerization of L,L-lactide has been used in order to prepare a highly-filled nanocomposite, which has been then redispersed in preformed PLA matrix or plasticized PLA matrix. Such a process, called “masterbatch technique,” has been envisaged in order to enhance the compatibility between the clay and the polymer matrix, and therefore to induce a better clay dispersion by the melt blending techniques.

Moreover, in situ intercalative polymerization of L,L-lactide has been conducted in presence of dihydroxylated PEG 1000 in order to generate triblock copolymers directly in the interlayer spacing of the organomodified silicate layers.

Experimental Part

Materials

L,L-Lactide was purchased from Boehringer Ingelheim and recrystallized three times in dried toluene (20 wt.-%/v) before use. Triethylaluminium (AlEt_3) and tin (II) octoate ($\text{Sn}(\text{Oct})_2$) solutions, from Fluka and Goldschmidt, respectively, were diluted in dried toluene and stored under nitrogen atmosphere into glass ampoules. PEG ($\bar{M}_w = 1000$) (PEG 1000) was supplied by Fluka and recrystallized three times in dried toluene

(20 wt.-%/v) before use. Three different clays were used and were supplied by Southern Clay Products (Texas, USA). Cloisite[®]Na⁺ corresponds to the natural unmodified montmorillonite-Na⁺. Cloisite[®]25A is a montmorillonite modified with dimethyl 2-ethylhexyl (hydrogenated tallowalkyl) ammonium cations, while Cloisite[®]30B is modified with bis-(2-hydroxyethyl) methyl tallowalkyl ammonium cations. The amount of organic materials in the organomodified clays was determined by thermogravimetric analysis as 26.9 wt.-% of organic materials for Cloisite[®]25A and 20.1 wt.-% for Cloisite[®]30B. Finally, poly(D,L-lactide) (70/30 L/D unity, $\bar{M}_n = 85\,000$, $\bar{M}_w/\bar{M}_n = 1.9$) was supplied by Cargill-Dow S.A.

Polymerization Process

Before synthesis, the aluminosilicate nanofillers were dried overnight at 70 °C in a ventilated oven, and then at the same temperature under reduced pressure for at least 3.5 h, directly in a flame-dried polymerization vial flask equipped with a three-way stopcock capped by a rubber septum. In parallel, the L,L-lactide monomer (and PEG 1000 when necessary) was purified by three successive crystallizations in dried toluene (20 wt.-%/v) in a separated, previously flame-dried, and nitrogen-purged round-bottom flask also equipped with a three-way stopcock capped by a rubber septum. The initiator/activator solution, followed by the monomer (and PEG 1000 when needed) in dried THF solution (30 wt.-%/v) were then added under nitrogen flow to the reaction vial and the solvent was eliminated under reduced pressure. Polymerizations were conducted in bulk at 120 °C, generally for 48 h. At the end of reaction time, the medium was quenched in liquid nitrogen and recovered by breaking the vial.

Masterbatch Process

In a first step, a highly filled Cloisite[®]30B/P(L-LA) nanocomposite (53 wt.-% in inorganic components) was prepared by in situ polymerization following the previously cited procedure. After the synthesis, a part of such masterbatch was then redispersed into commercial P(D,L-LA) in the molten state using a Brabender counter-rotating internal mixer, in order to reach a global inorganic content of 3 wt.-%. More precisely, the blending step was conducted in the presence of 0.3 wt.-% of Ultrinox[®]626 stabilizer with a rotation speed of 20 rpm for 4 min and then at 60 rpm for 3 min. The processing temperature was set at 180 °C, but it increased to 190 °C upon mixing. 3-mm thick plates were then shaped by compression moulding at 180 °C. The material was pressed under 150 bar for 120 s, followed by a cycle where the pressure was kept successively at 20, 80, 140 bar for 5 s and then released for 1 s after each pressure moulding increase (in order to get rid of any bubbles), and finally under 30 bar for 240 s. The sample was then cooled down by compressing at 15 °C under 30 bar for 5 min.

Characterization

Thermogravimetric analyses were performed using a Hi-Res TGA 2950 thermogravimetric analyzer from TA instrument

with a heating ramp of $20 \text{ K} \cdot \text{min}^{-1}$ under air flow ($74 \text{ cm}^3 \cdot \text{min}^{-1}$) from room temperature to 600°C .

Thermal behavior was measured with a DSC 2920 from TA instruments, with a heating and cooling ramp of $10 \text{ K} \cdot \text{min}^{-1}$ from -50°C to 200°C under nitrogen flow and the values were recorded during the second heating scan. The morphological analysis by X-ray diffraction was performed on a Siemens D5000 diffractometer using $\text{Cu}(K_\alpha)$ radiation (wavelength: 1.5406 \AA) at room temperature in the range of $2\theta = 1.5\text{--}30^\circ$ with a scanning rate of $2^\circ \cdot \text{min}^{-1}$. Molecular weight determination of PLA was carried out after eliminating the clay by cationic exchange reaction with LiCl . First a crude nanocomposite sample was dissolved in chloroform and then treated for 48 h with an equal volume of a 1 wt.-% aqueous LiCl solution. The chloroform phase was then centrifuged at 3000 rpm for 30 min in order to separate the polymer solution from the nanofiller. P(L,L-LA) chains were recovered by precipitation in a seven-fold volume excess of cold methanol (or heptane) and dried under vacuum at 60°C until constant weight. The Sn-based catalyst residues were removed by liquid-liquid extraction with a 0.1 M HCl aqueous solution and PLA was recovered by precipitation from cold methanol. For eliminating the Al-based catalyst residues, a liquid-liquid extraction was carried out using a 0.5 M aqueous solution of ethylenediaminetetraacetic acid at pH 4.8. Size-exclusion chromatography (SEC) measurements were performed in THF (added with 2 vol.-% of triethylamine) at 35°C using a Polymer Laboratory (PL) liquid chromatograph equipped with a PL-DG802 degazer, an isocratic HPLC pump LC1120 (flow rate: $1 \text{ ml} \cdot \text{min}^{-1}$), a Basic-Marathon autosampler, a PL-RI refractive index detector, and four columns: a guard column PLgel $10 \mu\text{m}$ ($50 \times 7.5 \text{ mm}$) and three columns PLgel $10 \mu\text{m}$ mixed-B ($300 \times 7.5 \text{ mm}$). Molecular weights and molecular distributions were calculated by reference to a universal calibration curve relative to PS standard, and using the Kuhn-Mark-Houwink equation for PLA in THF: $\bar{M}_n(\text{PLA}) = 0.4055 \times \bar{M}_n(\text{PS})^{1.0486}$.^[14]

For ^1H NMR analyses, the samples were prepared by introducing 30 mg of polymer chains extracted from the composites in 0.6 ml of deuterated chloroform (added with 0.03% of tetramethylsilane). The used spectrometer was a Bruker AMX-300 working at a frequency of 300 MHz for proton in a magnetic field of 7 T.

TEM observations were performed on two distinct equipments. The first was a Philips CM100 apparatus using an acceleration voltage of 100 kV. Ultrathin section of nanocomposite (ca. 80 nm) were prepared by ultramicrotomy at -130°C (Reichert-Jung Ultracut 3E, FC4E ultra-cryomicrotome equipped with a diamond knife). The second one was a Philips CM200 apparatus using also an acceleration voltage of 100 kV. Before analyses, the samples were cut in sections

between 75 and 90 nm of thickness using an ultra-cryomicrotome Leica UCT at -130°C .

Results and Discussion

Poly(L,L-lactide) (P(L,L-LA)) layered silicate (nano)compositions were prepared in bulk (i.e., in the absence of solvent) by intercalative in situ polymerization of L,L-lactide directly in the presence of montmorillonite, organo-modified or not. Three different layered clays were used, the unmodified natural montmorillonite Cloisite[®]Na⁺ and two organomodified clays, referred as Cloisite[®]25A and Cloisite[®]30B. Their characteristics in term of alkylammonium cation nature, relative content, as well as interlayer distance as determined by XRD are presented in Table 1.

Influence of the Alkylammonium Cation

Molecular Parameters and Polymerization Mechanism

In the first approach, in situ polymerization of L,L-lactide has been conducted in bulk in the presence of a fixed amount of (organo-)clays (3 wt.-% in inorganics), in order to understand the influence of the alkylammonium cation on the resulting composite morphology.

Practically, aluminium triisopropoxide ($\text{Al}(\text{O}^i\text{Pr})_3$) was used as initiator. Indeed, this aluminium alkoxide derivative is known to promote the polymerization of lactide, proceeding via a controlled "coordination-insertion" mechanism.^[15] More precisely, the experiments were carried out starting with an initial monomer-to- $\text{Al}(\text{O}^i\text{Pr})_3$ molar ratio equal to 300. The synthetic approach involved the dispersion of the layered silicates in the molten monomer, followed by the addition of the initiator. All the considered polymerizations were conducted at 120°C for 48 h. It has to be noted that, contrary to Cloisite[®]Na⁺ or Cloisite[®]25A, for which the initiation step is selectively promoted by the alkoxide groups of $\text{Al}(\text{O}^i\text{Pr})_3$ in the case of Cloisite[®]30B, the hydroxyl groups of the alkylammonium cations substituting the filler can also participate in the initiation step, through an exchange reaction between alcohol functions of the ammonium and alkoxide groups of $\text{Al}(\text{O}^i\text{Pr})_3$. Table 2 presents the experimental parameters and the composition of the so-obtained nanocomposites.

Table 1. Characteristics of used montmorillonites.

Filler	Exchanging cation	Organic fraction	Interlayer distance
		wt.-%	\AA
Cloisite [®] Na ⁺	Na ⁺	–	12.1
Cloisite [®] 30B	$(\text{C}_{18}\text{H}_{35})\text{N}^+(\text{C}_2\text{H}_4\text{OH})_2\text{CH}_3$	20.1	18.4
Cloisite [®] 25A	$(\text{C}_{18}\text{-H}_{37})\text{N}^+(\text{CH}_2\text{--CH}(\text{C}_2\text{H}_5)\text{--C}_3\text{H}_8)(\text{CH}_3)_2$	26.9	20.4

Table 2. Al(OⁱPr)₃ promoted polymerization of L,L-lactide in presence of 3 wt.-% of (organo-) clay (in bulk, 120 °C, 48 h).

Code	Clay	$n_{L,L-LA}/n_{Al}$	n_{OH}/n_{Al} ^{a)}	Conv. ^{b)}	DP_{th}	\bar{M}_n th ^{e)}	\bar{M}_n exp ^{f)}	\bar{M}_w/\bar{M}_n
				%		$g \cdot mol^{-1}$	$g \cdot mol^{-1}$	
SN3Na	Cloisite [®] Na ⁺	300	–	100	100 ^{c)}	14 400	16 500	1.5
SN3A25	Cloisite [®] 25A	300	–	100	100 ^{c)}	14 400	14 500	1.2
SN3B30	Cloisite [®] 30B	300	1.8	100	35 ^{d)}	5 040	5 400	1.2

^{a)} $n_{OH} = m_{clay} \times \text{organic content (in \%)} \times 2/MW$ (ammonium cations).

^{b)} As determined by gravimetry after extraction of clay and catalytic residues.

^{c)} $DP_{th} = [L,L-LA]_0 / \{[Al] \times 3\} \times \text{conv.}$

^{d)} $DP_{th} = [L,L-LA]_0 / \{[Al] \times 3 + [OH]_0\} \times \text{conv.}$

^{e)} \bar{M}_n th = $DP_{th} \times 144$.

^{f)} As determined by size-exclusion chromatography (SEC).

After extraction of both clays and aluminium residues (see *Experimental Part*) the recovered P(L,L-LA) chains have been characterized by SEC. As shown in Table 2, the experimental \bar{M}_n s are in agreement with the theoretical values. It seems therefore that the polymerization proceeds again through a controlled mechanism. Moreover, the polydispersity indices remain relatively narrow for such polymerization reactions conducted under heterogeneous conditions, i.e., in presence of (organo-)clay.

The possibility to directly graft the PLA chains on the surface of the organoclay through activation of hydroxyl groups borne by the ammonium cation of Cloisite[®]30B has prompted us to study the influence of the n_{OH}/n_{Al} initial molar ratio on its ability to promote the controlled polymerization.^[15] Accordingly, the relative content in Al(OⁱPr)₃ has been reduced while keeping the L,L-LA/clay ratio (3 wt.-%) constant. The results are gathered and shown in Table 3.

Clearly, a n_{OH}/n_{Al} molar ratio as high as 20 is responsible for some loss of control, as evidenced by the difference between theoretical and experimental \bar{M}_n s and broadening of the molecular weight distribution. It must be noted that most of the initiating species are actually issued from the organoclay itself, i.e., the filler (hydroxyl groups from Cloisite[®]30B). A possible explanation to this lack of polymerization control could stand in the partial deactivation of

the aluminium alkoxides by protic impurities associated to Cloisite[®]30B, actually in relatively larger quantity with regard to Al(OⁱPr)₃.

In order to know if the control in the polymerization process is function of the initiator nature, experiments have been performed considering only Cloisite[®]30B and two different activators, namely AlEt₃ and stannous (II) octoate (Sn(Oct)₂) for various molar ratios compared to the hydroxyl functions of the nanofiller (Table 4). Therefore, the initiation reaction will occur exclusively from the hydroxyl groups of the layered silicates, after their activation in alkoxide species by reaction with AlEt₃ or Sn(Oct)₂.^[16] The polymerization mechanism implies the coordination of the cyclic ester to the metallic atom, followed by the monomer insertion within the metal (Al or Sn) alkoxide bond by cleavage of endocyclic acyl-oxygen bond, in such way that the growing PLA chains remain attached to the metallic atom through an alkoxide bond.

Considering AlEt₃ as initiator precursor (first two entries in Table 4), the n_{OH}/n_{Al} molar ratio has been fixed firstly to 1 in order to form diethyl aluminium monoalkoxides by in situ reaction with the hydroxyl groups of the ammonium cations (Figure 1). By increasing the relative amount of AlEt₃, a n_{OH}/n_{Al} molar ratio of 3 has been then envisaged in order to form ideally aluminium trialkoxides as the initiating species at least.

Table 3. Influence of the n_{OH}/n_{Al} initial molar ratio on the in situ polymerization of L,L-lactide promoted by Al(OⁱPr)₃ in presence of 3 wt.-% of Cloisite[®]30B (in bulk, 120 °C, 48 h).

Code	$n_{L,L-LA}/n_{Al}$	n_{OH} ^{a)} / n_{Al}	Conv. ^{b)}	DP_{th} ^{c)}	\bar{M}_n th ^{d)}	\bar{M}_n exp ^{e)}	\bar{M}_w/\bar{M}_n
			%		$g \cdot mol^{-1}$	$g \cdot mol^{-1}$	
SN3B30(I)	300	1.8	100	35	5 040	5 400	1.2
SN3B30(II)	3 640	20	100	58	8 350	6 600	1.6

^{a)} $n_{OH} = m_{clay} \times \text{organic content (in \%)} \times 2/MW$ (ammonium cations).

^{b)} As determined by gravimetry after extraction of clay and catalytic residues.

^{c)} $DP_{th} = [L,L-LA]_0 / \{[Al] \times 3 + [OH]_0\} \times \text{conv.}$

^{d)} \bar{M}_n th = $DP_{th} \times 144$.

^{e)} As determined by SEC.

Table 4. Influence of triethylaluminium (AlEt₃) or tin (II) octoate (Sn(Oct)₂) as activator on the L,L-lactide polymerization in bulk in presence of 3 wt.-% of Cloisite[®]30B (in bulk, 120 °C, 48 h).

Code	Activator	$n_{\text{OH}}^{\text{a)}}$ / n_{Met}	Conv. ^{b)}	$DP_{\text{th}}^{\text{c)}$	$\bar{M}_n^{\text{th}^{\text{d)}}$	$\bar{M}_n^{\text{exp}^{\text{e)}}$	\bar{M}_w/\bar{M}_n
			%		$\text{g} \cdot \text{mol}^{-1}$	$\text{g} \cdot \text{mol}^{-1}$	
N3B30A11	AlEt ₃	1	85	142	20 500	10 300	1.7
N3B30A13	AlEt ₃	3	23	41	6 000	Bimodal ^{f)}	Bimodal ^{f)}
N3B30Sn1	Sn(Oct) ₂	1	71	120	17 280	14 100	2.4
N3B30Sn2	Sn(Oct) ₂	2	94	160	23 000	11 600	2.4

^{a)} $n_{\text{OH}} = m_{\text{clay}} \times \text{organic content (in \%)} \times 2/\text{MW (ammonium cations)}$.

^{b)} As determined by gravimetry after extraction of clay and catalytic residues.

^{c)} $DP_{\text{th}} = [\text{L,L-LA}]_0/[\text{OH}]_0 \times \text{conv.}$

^{d)} $\bar{M}_n^{\text{th}} = DP_{\text{th}} \times 144$.

^{e)} As determined by SEC.

^{f)} Bimodal distribution.

From the conversion, it can be deduced that the polymerization rate is function of the aluminium alkoxide nature that initiates the reaction. Indeed, the polymerization kinetics is much more rapid, when aluminium monoalkoxides are concerned, in comparison to trialkoxides. This behavior is in opposition to results obtained for the polymerization in solution or in homogeneous conditions (in bulk) of L,L-lactide. Indeed, Barakat et al. have shown that aluminium trialkoxides were able to promote L,L-LA polymerization in a controlled way with a much higher rate than diethyl aluminium monoalkoxide species.^[17] Such a

discrepancy can be explained by the difficulty to form aluminium trialkoxide species by reacting AlEt₃ with the dihydroxylated ammoniums species, actually ionically anchored on the clay surface of Cloisite[®]30B. Indeed, owing to the specific structure of Cloisite[®]30B interlayer spacing, the probability to form a large amount of trialkoxide species is rather low (Figure 2). Most probably, a mixture of aluminium mono-, di-, and tri-alkoxides is formed, which is responsible for the low monomer conversion, the loss of polymerization control and the bimodality of the molecular weight distribution. The experimental \bar{M}_n s greatly diverge

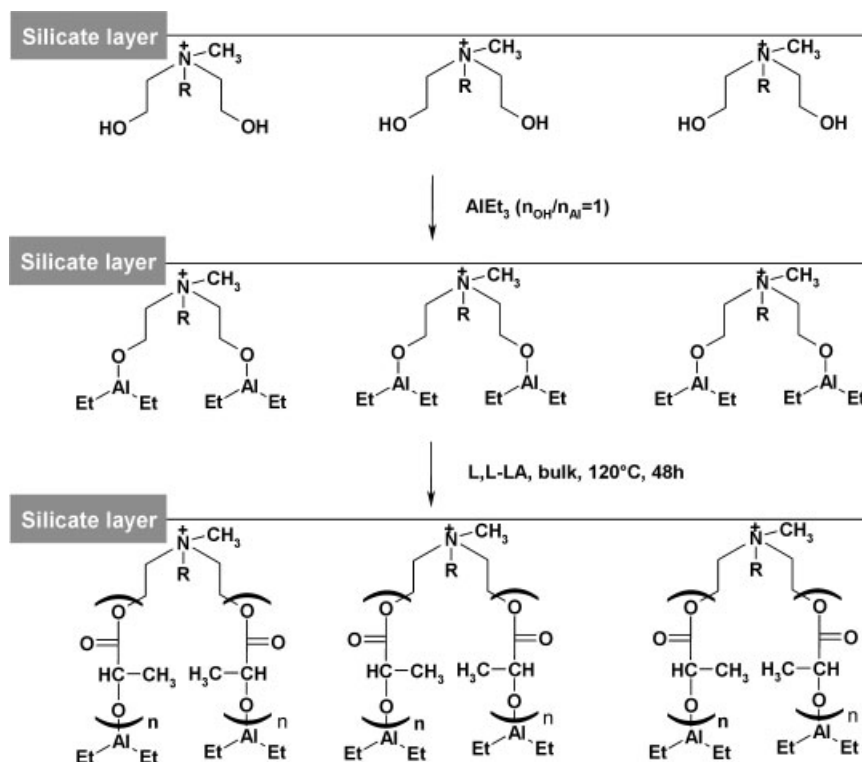


Figure 1. Schematic representation of the L,L-lactide polymerization performed in situ from Cloisite[®]30B using triethylaluminium (AlEt₃) as initiator (R stands for tallow alkyl chain).

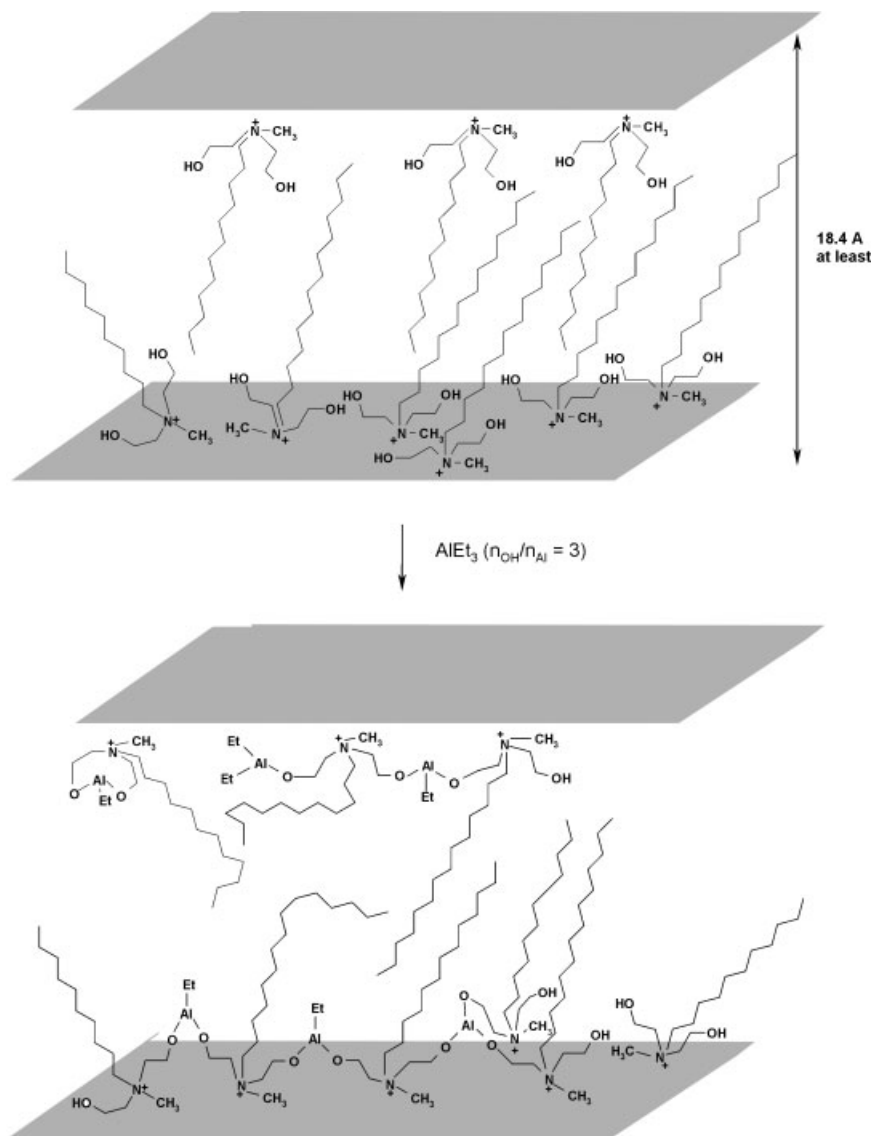
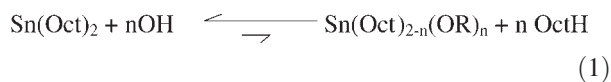


Figure 2. Sketch of some of the various aluminium alkoxides species that can be obtained when adding AlEt_3 onto Cloisite[®] 30B ($n_{\text{OH}}/n_{\text{Al}} = 3$).

from the theoretical values, whatever the initial $n_{\text{OH}}/n_{\text{Al}}$ molar ratio (Table 4).

In parallel, $\text{Sn}(\text{Oct})_2$ has been approached, as well the $n_{\text{OH}}/n_{\text{Sn}}$ molar ratio has been fixed from 1 to 2 (Table 4), while keeping the organomodified clay-to-monomer ratio constant. The in situ formation of tin alkoxide active species through the following equilibrium (Equation (1)) has been proposed for taking into account the polymerization activity of $\text{Sn}(\text{Oct})_2$ in the presence of alcohol (n_{OH}):^[11]



Even though the polymerization occurs smoothly with a lactide conversion higher than 90% after 24 h at 120 °C (for $n_{\text{OH}}/n_{\text{Sn}} = 2$), it appears that no control over the polymer-

ization could be reached. In conclusion, these results therefore bring the evidence that the results obtained for the polymerization of a lactone in some defined conditions cannot be directly extended to another lactone. Indeed, while ϵ -caprolactone can be polymerized in a perfectly controlled way in presence of clay and using different activators like tin octoate or AlEt_3 it is not the case for L,L-lactide, at least within the investigated experimental conditions.^[12,18]

Morphology

WAXS analyses were performed in order to characterize the morphology of the obtained composites prepared by in situ intercalative polymerization of L,L-lactide initiated by $\text{Al}(\text{O}^i\text{Pr})_3$.

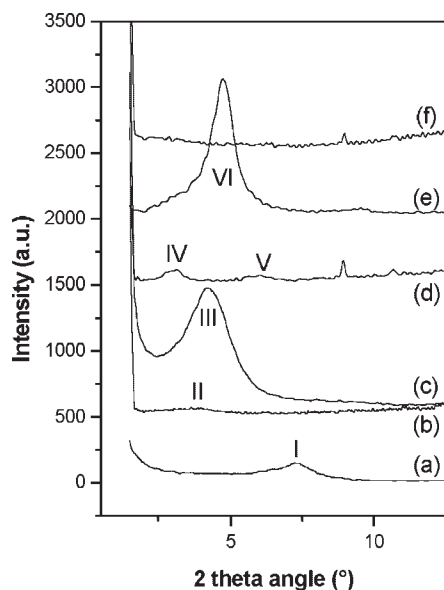


Figure 3. WAXS diffractograms of Cloisite[®]Na⁺ (curve (a)), Cloisite[®]25A (curve (c)), Cloisite[®]30B (curve (e)), and the related nanocomposites (each filled with 3 wt.-% inorganics) prepared by in situ intercalative polymerization of L,L-LA initiated by Al(OⁱPr)₃ (curves (b), (d), and (f), respectively); I is noted for interlayer distance $d_{(001)}$ of 12.0 Å, II for $d_{(001)}$ of 22.9 Å, III for $d_{(001)}$ of 20.4 Å, IV for $d_{(001)}$ of 28.3 Å, V for $d_{(002)}$ of 14.5 Å, and VI for $d_{(001)}$ of 18.4 Å.

As shown in Figure 3, both Cloisite[®]25A and Cloisite[®]Na⁺ led to intercalated nanocomposites. As far as Cloisite[®]Na⁺ is concerned, in situ polymerization allows to prepare an intercalated nanocomposite while only microcomposites could be recovered by direct melt-blending a preformed PLA matrix with the same pristine (non modified) clay.^[19] An explanation can stand in the swelling step of the layered silicates in the molten monomer before performing the initiation, so that the PLA chains can grow directly in the interlayer space of the clay. Such intercalation of a lactone monomer in the interlayer spacing of a Na⁺-montmorillonite has already been reported both theoretically and experimentally for ϵ -caprolactone.^[11,20]

When the in situ intercalative polymerization of L,L-lactide is carried out in presence of Cloisite[®]30B, no diffraction peak can be detected by WAXS (compare curves (e) and (f) in Figure 3). Such a result suggests the formation of an exfoliated structure and was confirmed by TEM as recently reported in our first communication.^[20] In this case, exfoliation is thus favored by the PLA chains grafting on the alkylammonium cations of the nanofiller, through their hydroxyl groups (as sketched in Figure 1).

Thermal and Crystallization Behavior

The thermal degradation behavior of nanocomposites based on 3 wt.-% of natural or organomodified montmorillonites

prepared by in situ intercalative polymerization of L,L-lactide initiated by Al(OⁱPr)₃ was studied by thermogravimetric analysis. Figure 4 shows the thermograms recorded under air flow for the nanocomposites based on Cloisite[®]Na⁺, Cloisite[®]25A and Cloisite[®]30B (3 wt.-% in inorganics) as well as for the P(L,L-LA) matrix extracted from the Cloisite[®]25A-based nanomaterials (see *Experimental Part*). Both intercalated and exfoliated nanocomposites degraded at higher temperatures compared to the selectively extracted PLA chains.

The temperature at which 50% weight loss is recorded increases in the following order: unfilled PLA < intercalated PLA/Cloisite[®]Na⁺ < intercalated PLA/Cloisite[®]25A < exfoliated PLA/Cloisite[®]30B. When intercalation of PLA chains takes place between clay platelets, a significant difference in thermal degradation can be observed between Cloisite[®]Na⁺ (Figure 4, curve (b)) and Cloisite[®]25A-based (Figure 4, curve (c)) nanocomposites. Indeed, the lower delay in degradation is noted for the natural sodium montmorillonite. This difference may rely on either a less regular and extended clay platelet intercalation for Cloisite[®]Na⁺ compared to Cloisite[®]25A or an effect from the absence of organomodifier within Cloisite[®]Na⁺ based nanocomposite. Thus, the thermal degradation for the nanocomposite based on Cloisite[®]30B arises at a higher temperature (temperature at which 50 wt.-% loss is recorded: 362 °C compared to 325 °C for unfilled P(L,L-LA). This increase in thermal stability occurs while the molecular weight of the P(L,L-LA) chains, surface-grafted to Cloisite[®]30B, is much lower ($\bar{M}_n = 5,400$) than those measured for the P(L,L-LA) matrix formed in presence of Cloisite[®]Na⁺ or 25A ($\bar{M}_n \sim 15,000$, see Table 2). This

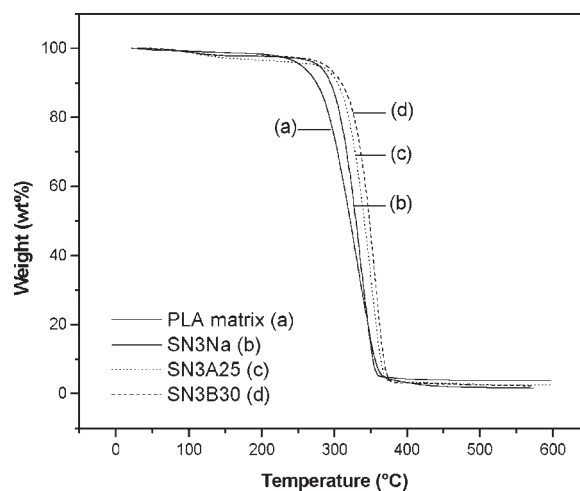


Figure 4. Temperature dependence of weight loss for nanocomposites containing 3 wt.-% (relative to inorganics) of (b) Cloisite[®]Na⁺, (c) Cloisite[®]25A, and (d) Cloisite[®]30B, directly compared to the PLA matrix (a) as recovered after extraction from the nanocomposite (c) (heating rate of 20 °C · min⁻¹, under air flow).

behavior has to be assigned both to clay layer delamination and P(L,L-LA) chain grafting onto the clay surface.^[13]

Finally, DSC analysis reveals, as was already observed for nanocomposites prepared by direct melt blending,^[19] that the nature of the clay organomodification does not affect neither T_g nor T_m values of the PLA chains, standing around 62 and 170 °C, respectively. As far the melting enthalpy is concerned, a value of ca. 55 J · g⁻¹ was found, whatever the nature of the filler.

Influence of Clay Loading

By using the in situ polymerization technique, it has been previously shown that intercalation or exfoliation of the clay platelets in the P(L,L-LA) matrix can be achieved in function of the organomodification of the aluminosilicates. In order to study the influence of the clay loading on nanocomposite morphology, we have focused our attention on Cloisite[®]25A, leading to intercalated species, and on Cloisite[®]30B, giving exfoliated nanocomposites, at least at 3 wt.-% in inorganic. Practically, in situ intercalative polymerizations of L,L-lactide were conducted in bulk, using Sn(Oct)₂ ($n_{L,L-LA}/n_{Sn} = 300$) as activator when Cloisite[®]25A was concerned, and AlEt₃ ($n_{OH}/n_{Al} = 1$) as aluminium alkoxide precursor for Cloisite[®]30B-based experiments. It must be noted that all the experimental conditions were adapted in function of the filler nature with the aim to reach 100% of conversion while tentatively limiting transesterification reactions. It has been therefore decided to conduct in situ polymerization at 120 °C for 24 h as far as Sn(Oct)₂ was concerned and for 48 h when AlEt₃ was used as activator. Table 5 presents the initial experimental conditions of the considered in situ polymerization and the molecular parameters of the extracted PLA chains.

Concerning the polyester chains issued from the nanocomposites based on Cloisite[®]25A (Table 5), the molecular weights remain relatively constant (around 38 000 as \bar{M}_n) whatever the clay content. It can, therefore, be concluded that both the clay and the alkylammonium cation of this filler behave as spectator entities in the initiation and propagation processes.

On the contrary, when the relative content in Cloisite[®]30B is increased, the concentration in hydroxyl functions in the medium is consequently higher, which should lead to P(L,L-LA) grafts characterized by a lower degree of polymerization. Monomer conversion (Table 5) does not seem to be complete, which is actually in discrepancy with TGA results (see hereafter). Indeed, one cannot preclude an under-estimation of the conversion due to some fractionation as the polyester chains were recovered by precipitation from cold methanol, a solvent for the monomer but also for P(L,L-LA) oligomers. When considering polyesters chains formed in nanocomposites containing 1 or 3 wt.-% of Cloisite[®]30B, the experimental molecular weight of the extracted PLA obtained by SEC differs significantly from the predicted ones on the basis of the hydroxyl content in the reaction medium. However, when the in situ polymerization of L,L-lactide is conducted in the presence of 5 wt.-% of Cloisite[®]30B, a relatively good agreement between experimental and theoretical PLA molecular weights is found. Such a discrepancy might find some explanation in the investigated PLA extraction process, i.e., an ionic exchange reaction between the ammonium cations bearing the PLA grafts and lithium cations (see *Experimental Part*). It appears that this technique, thus used for eliminating the silicate layers from the polymer chains, is more adapted to shorter polyester chains. As the chains length increases, the accessibility to cationic sites of the layered silicates is more

Table 5. Influence of the clay content on monomer conversion and molecular parameters of the P(L,L-LA) chains extracted from nanocomposites based on Cloisite[®]25A and Cloisite[®]30B (in bulk, 120 °C, 48 h) and their thermal transitions and melting temperature.

Code	Clay		Conv. ^{a)} %	\bar{M}_n th ^{b)} g · mol ⁻¹	\bar{M}_n exp ^{c)} g · mol ⁻¹	\bar{M}_w/\bar{M}_n	T_g ^{f)} °C	T_m ^{f)} °C	ΔH_m ^{f)} J · g ⁻¹
	Type	wt.-%							
SN1A25	Cloisite [®] 25A ^{d)}	1	99	–	35 300	>2	55	170	39.7
SN3A25		3	98	–	40 000	>2	62	172	35.1
SN5A25		5	97	–	39 000	>2	62	170	29.8
SN10A25	Cloisite [®] 30B ^{e)}	10	98	–	36 000	~2	62	171	39.4
SN1B30		1	81	64 800	17 800	~2	60	180	61.8
SN3B30		3	85	20 500	10 300	1.7	62	173	55.6
SN5B30		5	87	13 100	14 000	1.9	60	174	42.4
SN10B30		10	93	6 600	ND	ND	61	170	42.6

^{a)} As determined by gravimetry after extraction of clay and catalytic residues.

^{b)} \bar{M}_n th = $[L,L-LA]_0/[OH]_0 \times \text{conv.} \times 144$.

^{c)} As determined by SEC; polydispersity indices close to 2 in all entries (ND, not determined).

^{d)} Sn(Oct)₂ as promotor: $n_{L,L-LA}/n_{Sn} = 300$ (in bulk, 120 °C, 24 h).

^{e)} AlEt₃ as promotor: $n_{OH}/n_{Al} = 1$ (in bulk, 120 °C, 48 h).

^{f)} By DSC under nitrogen flow from –10 to 200 °C (10 °C · min⁻¹).

difficult for an alkaline cation such as lithium cation, leading to a less efficient extraction of the longer P(L,L-LA) chains.

In term of morphology, as revealed by WAXS analysis (Figure 5), intercalation of PLA chains into the interlayer spacing of Cloisite[®]25A is highlighted by a shift of $d_{(001)}$ peak of the organoclay (noted I in Figure 5) in the nanocomposite towards lower 2θ angles. As an example, considering a nanocomposite prepared from 5 wt.-% of Cloisite[®]25A, the interlayer distance $d_{(001)}$ in the nanocomposite (noted V in Figure 5) approaches 33 Å, while it has a value of 20.4 Å in the corresponding organoclay. Moreover, increasing the nanofiller content leads to a more precisely defined and narrow $d_{(001)}$ diffraction peak (noted II, III, V, and VII for 1, 3, 5, and 10 wt.-% Cloisite[®]25A, respectively) and better definition of $d_{(002)}$ diffraction peak (noted IV, VI, and VIII for 3, 5, and 10 wt.-% Cloisite[®]25A, respectively), as a consequence of more regular platelets stacking at higher clay content, for instance 10 wt.-% in inorganics. As far as Cloisite[®]30B-based nanocomposites are concerned, no trace of diffraction peak showing up at low 2θ angle can be observed on the XRD patterns (from 1 to 10 wt.-% in inorganics, Figure 6 where the dashed line and star show the localization of the diffraction peak for Cloisite[®]30B).

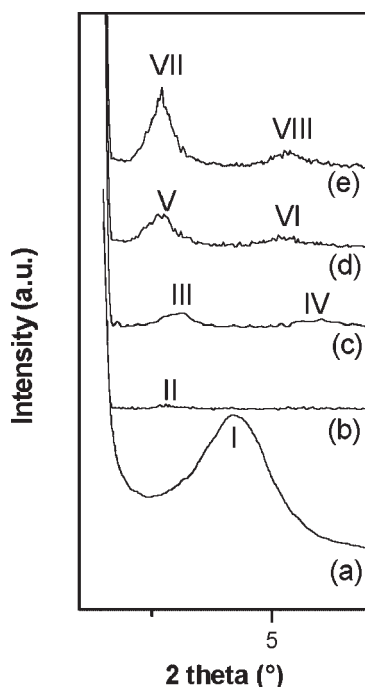


Figure 5. WAXS diffractograms of Cloisite[®]25A (curve (a)), and nanocomposites based on different amounts of filler, respectively 1 wt.-% (curve (b)), 3 wt.-% (curve (c)), 5 wt.-% (curve (d)), and 10 wt.-% (curve (e)); I is denoted for the interlayer distance $d_{(001)}$ corresponding to 20.4 Å, II for $d_{(001)}$ of 32.2 Å, III for $d_{(001)}$ of 28.3 Å, and IV for the $d_{(002)}$ corresponding to 14.5 Å; V for $d_{(001)}$ of 32.7 Å, and VI for $d_{(002)}$ of 16.7 Å, finally VII is noted for $d_{(001)}$ of 32.8 Å and VIII for $d_{(002)}$ of 16.5 Å.

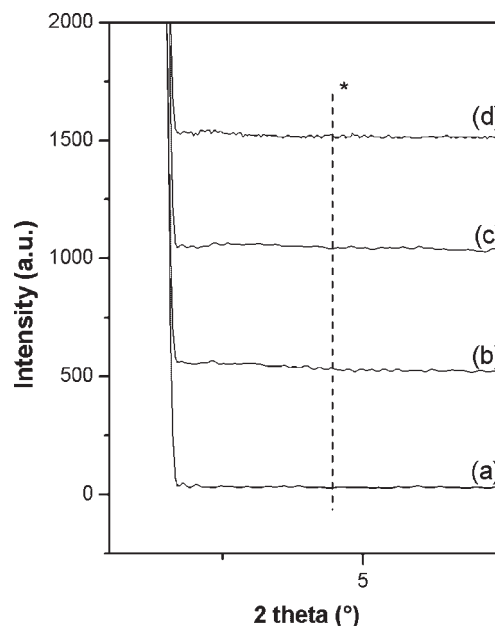


Figure 6. WAXS diffractograms of nanocomposites prepared by in situ polymerization and filled with 1 wt.-% (curve (a)), 3 wt.-% (curve (b)), 5 wt.-% (curve (c)), and 10 wt.-% (curve (d)) of Cloisite[®]30B (*shows the location of the interlayer distance $d_{(001)}$ for Cloisite[®]30B alone).

The thermal stability of the Cloisite[®]30B-based nanocomposites containing from 1 to 10 wt.-% nanoclay has been analyzed by TGA and compared with P(L,L-LA) extracted from 5 wt.-% Cloisite[®]30B nanocomposite ($\bar{M}_n \sim 14\,000$) (Figure 7). Whatever the filler content, these nanocomposites exhibit a better thermal stability than the unfilled matrix. Such a delay in the degradation temperature may be ascribed to a decrease in oxygen and volatile degradation products permeability/diffusivity due to the homogeneous dispersion/delamination of clay sheets, arising from the barrier properties of this high aspect ratio filler. Char formation is also responsible for such an increase in thermal stability.^[5] While the best thermal properties are observed for nanocomposites filled with 1 and 3 wt.-% of exfoliated Cloisite[®]30B, the temperature shift is less important when filled with 5 and 10 wt.-%. Two inter-related phenomena may be at the origin of this decrease. First, the extent of clay dispersion in PLA matrix decreases with the clay loading, as a result of sterical hindrance around the clay platelets, which are knocking each other at high filler loading. Another explanation relies upon the decrease in molecular weight of the grafted PLA chains, expected from the higher concentration in initiating species at higher Cloisite[®]30B content. Finally, no trace of residual monomer, characterized by a volatilization around 200 °C, can be observed attesting for the quantitative conversion of L,L-LA upon polymerization.

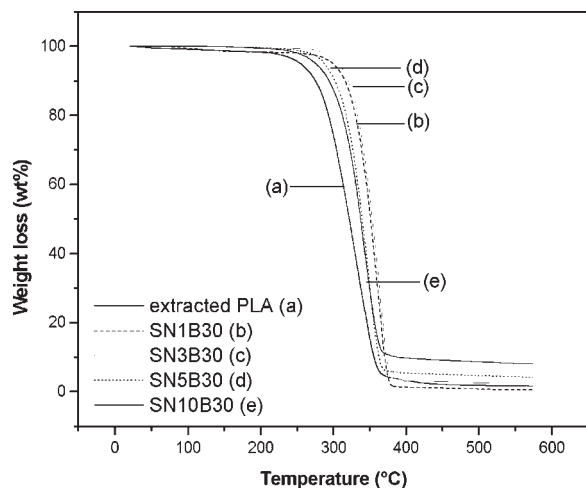


Figure 7. Thermogravimetric analysis of (a) extracted PLA ($M_n = 14\,000\text{ g}\cdot\text{mol}^{-1}$) and nanocomposites prepared by in situ intercalative polymerization of L,L-LA in presence of (b) 1, (c) 3, (d) 5, and (e) 10 wt.% of Cloisite[®]30B (under air flow using a heating ramp of $20\text{ }^\circ\text{C}\cdot\text{min}^{-1}$).

Finally, considering the nanocomposites based on Cloisite[®]25A, DSC analyses have shown that a filler content as low as 1 wt.% does not significantly influence the T_g of the matrix, as the thermal transition is kept closed to $55\text{ }^\circ\text{C}$ (Table 5). Indeed, T_g for a commercial P(L,L-LA) characterized by the same molecular mass has been detected around $55\text{ }^\circ\text{C}$, under the same analysis conditions. However, as the filler content increases from 3 to 10 wt.%, a slight increase in T_g has been evidenced and could be explained by the limitation of the chains relaxation following their intercalation in the interlayer spacing of the clay. The relatively low extent of intercalated polyester chains compared to completely free ones in the nanocomposites based on 1 wt.% in inorganics is probably the reason why such phenomenon is not observed at such a low loading. In addition, the T_m values of the polyester matrix chains are not influenced by the filler loading. In parallel, ΔH_m values have been kept relatively constant with the clay loading, the aluminosilicate platelets cannot be therefore considered as nucleating agents. As far as the Cloisite[®]30B based nanocomposites are concerned (Table 5), the decrease of the melting enthalpy at higher filler content could be related to the P(L,L-LA) chains length. Indeed, as the Cloisite[®]30B loading in the nanocomposites increases, the concentration of hydroxyl groups initiating the L,L-lactide polymerization increases in the same manner, leading to shorter P(L,L-LA) grafts, which need less thermal energy to melt. On the other hand, all the samples are characterized by a glass transition temperature as high as $61 \pm 1\text{ }^\circ\text{C}$, T_g typical for non-plasticized P(L,L-LA) chains. Such a value is consistent, once again, with a quantitative conversion of L,L-LA to P(L,L-LA), as lactide is known to be a good plasticizer for P(L,L-LA).

Masterbatch Process

Melt intercalation of preformed polymers and in situ intercalative polymerization are the two techniques most commonly used to prepare polymer/clay nanocomposites. The first method is effective whenever the thermodynamics of the molten polymer/organoclay pair allows the chains to crawl within the clay interlayer spaces, so pushing the individual sheets apart one from each other. The second method relies on the swelling of the organoclay by the liquid monomer (or by the molten monomer if solid) followed by the in situ polymerization initiated by a suitable compound. The chains growth in the clay galleries can trigger the clay exfoliation and the nanocomposite formation in case of adequately organomodified clays.

Knowing that the best improvement of the matrix properties is most often achieved by the complete delamination of the aluminosilicate layers, there is therefore a lot of interest to prepare exfoliated nanocomposites at large scale industrial production level. However, the in situ polymerization approach presents the major disadvantage to imply organometallic catalysts, degradation-sensitive monomer, and in some cases solvent(s), which could limit its (industrial) exploitation where the technique of melt intercalation is preferred.

For that purpose, another approach, combining both the in situ intercalative polymerization and the melt intercalation processes, has been envisaged. A highly-filled organomodified clay/PLA masterbatch is first prepared by in situ polymerization of L,L-lactide, followed by melt mixing it with commercially available PLA matrix (plasticized with PEG 1000 or not). The main advantage of this particular technique stands in the possibility to obtain nanocomposite with a high degree of exfoliation, which cannot be achieved by direct melt blending of the polyester with the clay.

This original process has already been used in order to prepare PCL and poly(vinyl chloride) (PVC) layered silicate nanocomposites.^[21] Highly-filled PCL masterbatches (with typical content of nanoclay in the range of 25–50 wt.%) were first prepared by the in situ ϵ -caprolactone polymerization. The masterbatches were then melt blended with either PCL or PVC (actually known to be miscible to PCL) such that the final clay content was lower than 10 wt.%. Depending on the alkylammonium cation used to modify the filler surface, exfoliated nanostructures have been evidenced by both WAXS and TEM. In addition, highly-loaded PCL/Cloisite[®]30B masterbatches have been recently studied for the preparation of nanocomposites based on poly(propylene), polystyrene, high impact polystyrene, polyethylene, and acrylonitrile-butadiene-styrene terpolymer.^[22] The PCL chains grafted on the filler were acting as compatibilizing agent between the filler and the tested matrices.

Based on these encouraging results, the masterbatch technique has been studied to prepare PLA-based nanocom-

posites containing 3 wt.-% of clay, dispersed in commercially available PLA and plasticized PLA. Both nanocomposites have been characterized in terms of morphology as well as thermal and crystallization behaviors.

Synthesis of P(L,L-LA)/Cloisite[®]30B Masterbatch

First of all, a P(L,L-LA) masterbatch based on high Cloisite[®]30B content has been prepared by ring-opening polymerization of L,L-lactide in bulk at 120 °C for 16 h, using AlEt₃ as activator ($n_{OH}/n_{Al} = 1$). An initial amount of approximately 30 wt.-% inorganic clay with respect to monomer was fixed, in order to ensure a relatively good dispersion of the layered aluminosilicates in the molten L,L-lactide. In order to recover a P(L,L-LA) composite highly loaded by Cloisite[®]30B, the polymerization time has been adapted to limit the monomer conversion. As L,L-lactide is one of the best known plasticizer for PLA chains, and knowing the brittleness of the PLA matrix in which the masterbatch has to be dispersed in a second step, residual monomer was not totally removed.

TGA analysis has been used to determine the final clay content of the masterbatch, which reached 53 wt.-% in clay. Unfortunately, due to the huge difficulty to quantitatively extract the clay and catalytic residues (by cationic exchange reaction and aqueous washing step) from the “grafted” P(L,L-LA) chains, it has not been possible to determine the experimental \bar{M}_n of the grafted P(L,L-LA) chains, neither by SEC nor NMR. However, knowing the clay loading (53 wt.-%) and assuming that all hydroxyl functions of the Cloisite[®]30B would have participated in the initiation step of polymerization, one can estimate an \bar{M}_n of ca. 1 400 (per PLA grafts).

In contrast to the exfoliated nanocomposites prepared by the same technique, i.e., in situ polymerization, but with a lower filler content (3 wt.-%), a perfectly intercalated structure has been evidenced for this highly-filled masterbatch, as revealed by the WAXS diffractogram compared with the diffraction peak of Cloisite[®]30B (noted I), as reported in Figure 8. Interestingly, the two successive registries of $d_{(001)}$ diffraction peak (corresponding to 34.5 Å and noted II), $d_{(002)}$ (noted III), and $d_{(003)}$ (noted IV), have also been detected by X-ray diffraction. They are indicative of a regular intercalated clay stacking.

Two parameters can explain this absence of exfoliation. First, for sterical reasons, the clay platelets exfoliation at high filler level is hindered by the limited volume remaining available for delamination of every silicate layer.^[11] Moreover, in order to exfoliate each clay platelet, the P(L,L-LA) chains, grafted by the in situ polymerization starting from the hydroxyl groups of the Cloisite[®]30B ammonium cations, have to be characterized by a molecular weight high enough to peel apart the layers. As the filler content is extremely high in the masterbatch, the quantity of hydroxyl groups able to promote the L,L-lactide polymerization is

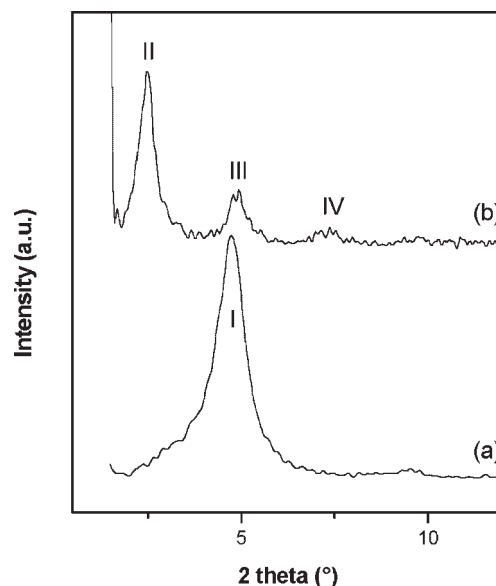


Figure 8. WAXS diffractograms of Cloisite[®]30B (curve (a)), for which I is noted for $d_{(001)}$ interlayer distance of 18.4 Å, and of a masterbatch PLA/Cloisite[®]30B (53 wt.-% in clay) (curve (b)), II is noted for $d_{(001)}$ of 34.5 Å, III for $d_{(002)}$ of 17.8 Å, and IV for $d_{(003)}$ of 11.9 Å.

also high, leading to P(L,L-LA) chains with a relatively low degree of polymerization (thus estimated to ca. 10). These chains, while being grafted to the aluminosilicate surface, remain therefore too short to imply a subsequent clay exfoliation.

(Plasticized) Poly(L-Lactide)/Cloisite[®]30B Nanocomposite(s) From Masterbatch Dispersion

Two nanocomposites, based on both pure PLA and PLA plasticized with 20 wt.-% of PEG 1000, have been prepared by melt blending a commercial PLA matrix (L/D 70/30, $\bar{M}_n = 85\,000$) with the previously synthesized Cloisite[®]30B-based masterbatch (thus filled with 53 wt.-% clay) in order to finally reach an inorganic loading of 3 wt.-%. As the aim of the technique is to improve exfoliation when compared to more conventional melt blending, both composites have been analyzed by WAXS and TEM in order to characterize the clay dispersion in the matrix as well as its dispersion. Figure 9 presents X-ray diffractograms recorded for the masterbatch (curve (a)) characterized by its diffraction peak $d_{(001)}$ and two registries $d_{(002)}$ and $d_{(003)}$ (noted I, II, and III, respectively), and the nanocomposite obtained by melt blending of this masterbatch within P(D,L-LA) matrix (curve (b)) and P(D,L-LA) plasticized with 20 wt.-% PEG 1000 (curve (c)).

Figure 9 indicates that the redispersion of the masterbatch based on Cloisite[®]30B into unplasticized PLA matrix seems, in a first interpretation, to lead to the dispersion of some regular stacking of clay platelets from the masterbatch itself but without increasing of the interlayer distance

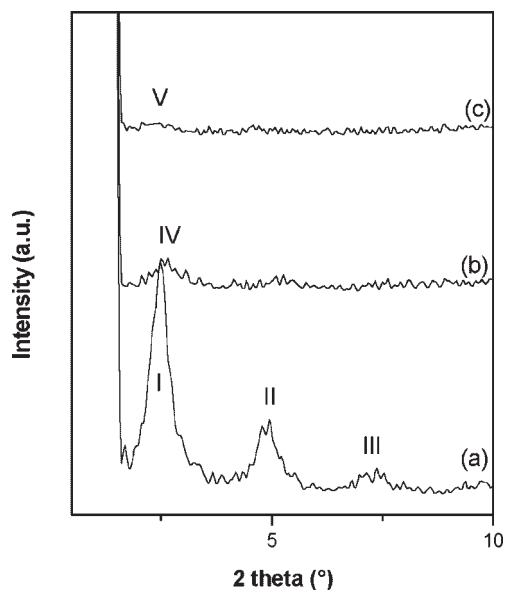


Figure 9. WAXS diffractograms of Cloisite[®] 30B-based masterbatch (curve (a)), the nanocomposite obtained by its melt blending within unplasticized poly(L,L-lactide) (P(L,L-LA)) (curve (b)) and within the plasticized polyester matrix (curve (c)); I stands for interlayer distance $d_{(001)}$ of 34.5 Å, II for $d_{(002)}$ of 17.8 Å, III for $d_{(003)}$ of 11.9 Å, IV for $d_{(001)}$ of 33.7 Å, and V for $d_{(001)}$ of 43.9 Å.

upon mixing. Indeed, the diffraction peak $d_{(001)}$ (noted IV), sited around 2.5° as 2θ angle, is relatively well defined and narrow, and stands closed to the $d_{(001)}$ initially attributed to the masterbatch. However, a TEM picture recorded for this nanocomposite (Figure 10) reveals that the nanofiller

platelets are extremely well dispersed and co-exist with a limited amount of intercalated stacks (more likely responsible for the diffraction around 2.5°). Clearly, the proposed masterbatch process allows for reaching high level of exfoliation while starting from a commercially available matrix.

Considering the plasticized P(D,L-LA)-based nanocomposite, a relatively weak and large $d_{(001)}$ diffraction peak (noted V) has been detected in the X-ray diffraction pattern (Figure 9, curve (c)), corresponding to an interlayer distance of 43.9 Å. Knowing that the two nanocompositions (based on unplasticized matrix and based on plasticized P(D,L-LA)) have been prepared using the same operating conditions, it appears that PEG 1000 seems to act as a second compatibilizer between the aluminosilicate layers and the polyester chains, the first one being the P(L,L-LA) grafts covering the clay surface. Indeed, the significant difference in interlayer spacing (ca. 10 Å) between the two nanocomposites, as well as a more diffuse diffraction curve are indicative for improved clay deconstruction.

In addition, it must be reminded that a direct melt blend of P(D,L-LA) with 20 wt.-% of PEG 1000 and 3 wt.-% of Cloisite[®] 30B gives intercalated structure characterized by an interlayer distance around 37.8 Å.^[4] The increase of the interlayer spacing up to 43.9 Å for the nanocomposite obtained by the masterbatch redispersion can therefore be explained by the compatibilizing effect between each blend components due to the grafting of short P(L,L-LA) chains directly on the silicate layers.

In term of crystallization behavior, the dispersion of montmorillonite in a PLA matrix through the masterbatch process does not affect the T_g of the polyester chains,

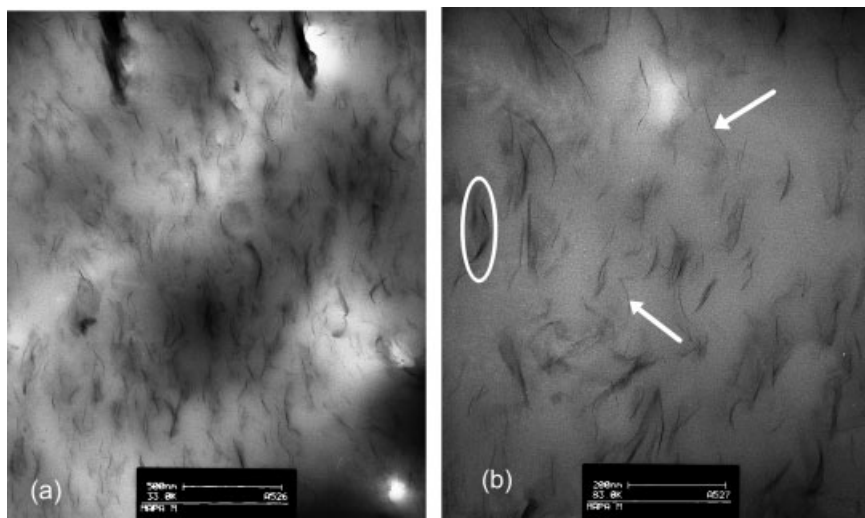


Figure 10. TEM pictures of a nanocomposite based on 3 wt.-% clay after redispersion of the highly-filled Cloisite[®] 30B-based masterbatch (53 wt.-% in clay), and presenting both fine dispersion of the filler (picture (a)) and delamination of platelets (picture (b)); individual layers are pointed out by arrows and intercalated stacking is surrounded in picture (b).

Table 6. Influence of masterbatch process on thermal and crystallization parameters of Cloisite[®]30B-based PLA nanocomposites.

Code	T_g	T_c	ΔH_c	T_m	ΔH_m
	°C	°C	J · g ⁻¹	°C	J · g ⁻¹
N3B30 ^{a)}	58	–	–	–	–
N3B30m ^{b)}	61	–	–	153	1.4
pN3B30m ^{c)}	26	83	2.4	152	42.9

^{a)} N3B30 stands for the nanocomposite based on 3 wt.-% Cloisite[®]30B prepared by melt blending.

^{b)} N3B30m is noted for the nanocomposite prepared from the redispersion of the Cloisite[®]30 masterbatch in PLA matrix in order to reach a 3 wt.-% clay loading.

^{c)} pN3B30m is noted for the nanocomposite prepared from the redispersion of the Cloisite[®]30 masterbatch in plasticized (with 20 wt.-% PEG 1000) PLA matrix in order to reach a 3 wt.-% clay loading.

compared to direct melt blending of this filler with the P(L,L-LA) (Table 6). However, compared to the conventional melt blend where the P(L,L-LA) matrix remains totally amorphous, a relatively low ΔH_m can be detected for the masterbatch-based nanocomposite (N3B30m, Table 6) with a maximum near 153 °C. It seems that the short-chain P(L,L-LA) grafted Cloisite[®]30B can act as nucleating agents, however, with a limited action. Such effect is not observed for simply intercalated nanocomposites, leading to the conclusion that isolated (delaminated) clay platelets grafted with short P(L,L-LA) chains can trigger different and interesting properties to the P(L,L-LA) matrix. In parallel, when 20 wt.-% of PEG 1000 is involved in the nanocomposite preparation, the plasticizer decreases the T_g of the PLA matrix to 26 °C but, together with the delaminated aluminosilicate platelets, allows for increasing significantly the melting enthalpy with a ΔH_m up to 42.9 J · g⁻¹ and a cold crystallization taking place at 83 °C.

In situ Polymerization in Presence of PEG

Due to its relative brittleness, P(L,L-LA) thus needs to be plasticized in order to fulfill mechanical requirements, which will allow to extend its application domain. For that specific reason, we have been attached in a first approach to prepare nanocomposites by melt blending the P(L,L-LA) matrix and a selected plasticizer, PEG 1000, together with the nanofiller. However, as for most of the plasticizers, PEG 1000 tends to diffuse out of the material and accumulates at the nanocomposite surface, leading to structural matrix changes upon ageing.^[23,24] One attractive solution relies upon the *in situ* intercalative polymerization again carried out in bulk and directly in the presence of end-hydroxylated PEG 1000. This should lead to the polymerization of L,L-lactide as initiated by the hydroxyl end-groups of α,ω -diOH

PEG 1000 plasticizer, thus in presence of the organoclay. The as-synthesized P(L,L-LA)-b-PEG-b-P(L,L-LA) triblocks might lead to a better stabilization of the plasticizer within the materials.

Practically, as the best results in term of morphology as well as thermal behavior have been obtained for Cloisite[®]30B-based nanocomposites, it has been decided to study this organoclay directly in the presence of α,ω -diOH PEG 1000. Sn(Oct)₂ has been used as activator and added to the reaction medium in a n_{OH}/n_{Sn} molar ratio equal to 2, where n_{OH} takes into account hydroxyls groups from both PEG 1000 and Cloisite[®]30B. It must be noted that the n_{OH}/n_{Sn} molar ratio was fixed to 2 based on the results obtained for the homopolymerization of L,L-lactide conducted in the presence of 3 wt.-% of Cloisite[®]30B, which led to rather acceptable monomer conversion under the studied experimental conditions.

As a matter of fact, two types of hydroxyl groups co-exist in the reaction medium, i.e., those present on the ammonium cation that modifies the clay and the OH-end groups of the PEG chains. Different types of chains can therefore be formed: P(L,L-LA) homopolymers “grafted” to the silicate layers and P(L,L-LA)-b-EG-b-L,L-LA triblock copolymers more likely present as intercalated species within the organoclay galleries. The influence of the α,ω -diOH PEG 1000 amount for a constant filler content of Cloisite[®]30B (3 wt.-%) has been more closely studied. While keeping constant the loading in Cloisite[®]30B in the nanocomposite, different relative contents in α,ω -diOH PEG 1000, varying from ca. 1 to 16 wt.-%, have been added in order to vary the P(L,L-LA) sequence length in the triblock copolymers as well as for the surface-grafted P(L,L-LA) chains. In order to avoid any fractionation of the polyester chains upon P(L,L-LA) precipitation, heptane has been used as non-solvent (rather than methanol—known to precipitate P(L,L-LA) chains of higher molecular weight only) to recover the polyester chains after clay and metal residues extraction. ¹H NMR analysis of the extracted polymers has allowed to evaluate the monomer conversion, degree of polymerization, and weight fraction of PEG compared to *in situ* generated PLA (Table 7).

Quantitative conversion is assumed since no trace of residual monomer has been evidenced by ¹H NMR. Indeed, L,L-lactide being insoluble in heptane, the presence of any residual monomer would have been observed by ¹H NMR analysis.

In order to interpret the results, one has to remind previous observations for L,L-lactide polymerization in the presence of Cloisite[®]30B. It has been shown that when high $DP_{L,L-LA}$ were targeted, a large discrepancy between the theoretical and experimental values was observed, with much lower experimental $DP_{L,L-LA}$. This difference has been explained by the difficulty to exchange by Li⁺ cations the ammonium salts grafted with longer PLA sequences. As a result, only the shorter PLA chains were extracted and

Table 7. Influence of the PEG 1000 content on molecular parameters of in situ polymerized P(L,L-LA) in nanocomposites filled with 3 wt.-% Cloisite®30B (in bulk, 120 °C, 48 h, Sn(Oct)₂, $n_{\text{OH}}/n_{\text{Sn}} = 2$).

Code	PEG content	$n_{\text{OH}}(\text{PEG})/$ $n_{\text{OH}} \text{ total}$	Conv. ^{a)}	DP_{th} ^{b)}	DP_{exp} ^{c)}
	wt.-%		%		
SC1N3B30	0.8	0.28	100	114	28
SC5N3B30	4.4	0.69	100	50	23
SC10N3B30	8.5	0.82	100	29	19
SC20N3B30	16.2	0.91	100	16	14

^{a)} Determined by ¹H NMR.

^{b)} $DP_{\text{th}} = [\text{L,L-LA}]_0 / \{[\text{OH}]_{\text{PEG}} + [\text{OH}]_{\text{clay}}\} \times \text{conv.}$

^{c)} Determined by ¹H NMR using the relative intensity of the methine protons from the repetitive unit in the chain ($-\text{CH}(\text{Me})-\text{O}-\text{C}(\text{O})-$) and the end groups ($-\text{CH}(\text{Me})-\text{OH}$); $DP_{\text{exp}} = I_{\text{unit}}/I_{\text{end group}} \times 2$.

therefore analyzed by SEC, which led to an under-estimation of the actual molecular weight of the grafted PLA chains. A similar behavior seems to be observed in Table 7 where a better agreement between the theoretical and experimental $DP_{\text{L,L-LA}}$ values is obtained for the lower values of DP_{th} (entries 3 and 4).

As revealed by WAXS analyses (not shown here), the relative content in PEG 1000 does not affect the morphology of the resulting nanocomposites. Again, the complete disappearance of the diffraction peak characteristics of Cloisite®30B attests for the complete loss in the organization of the clay platelets.

TGA thermograms (Figure 11a, b) display two distinct degradation steps. Based on their relative importance, the first step has been assigned to the degradation of P(L,L-LA) sequences, while the second (occurring at higher temperature) can be attributed to more thermally stable PEG blocks. This attribution is fully confirmed by measuring the relative weight loss of the two consecutive degradations, which leads to a PEG content (PEG^{TGA}) in good agreement with the initial content in PEG (Table 8).^[25]

Finally, DSC analyses have revealed that the plasticizing effect of the PEG sequences in in situ polymerized triblock copolymers is only detectable for a PEG content of 8.5 wt.-% as attested by the decrease of the T_{g} (down to 41 °C). At ca. 16.2 wt.-% in PEG, a much more significant plasticizing effect has been evidenced with a T_{g} as low as 12 °C, which can be explained by a conjugated effect of high PEG content and the formation of very short P(L,L-LA) sequences ($DP_{\text{L,L-LA}} = 14$, entry 4 in Table 7).

Conclusion

In contrast to the melt blending technique, for which only intercalated P(L,L-LA)/nanocomposites can be recovered, the in situ polymerization of L,L-lactide in presence of

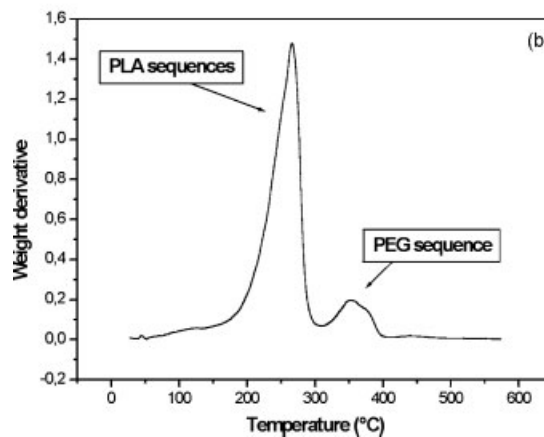
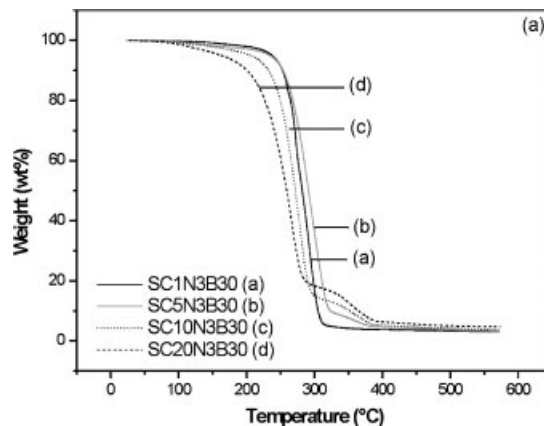


Figure 11. (a) TGA thermograms of nanocomposites filled with 3 wt.-% Cloisite®30B (noted 3B30) and prepared in the presence of 0.8, 4.4, 8.5, or 16.2 wt.-% of PEG 1000, respectively; (b) d-TGA curve of SC1N3B30 showing the two-step degradation (under air flow with a heating ramp of 20 °C · min⁻¹).

Cloisite®30B leads to exfoliated morphology. This nanostructure has been explained by the possibility to initiate the polymerization through activation of the hydroxyl groups covering the silicate layer surface. The good distribution/dispersion of the clay platelets, that directly arises from the polyester chains grafting, gives largely improved properties to the materials, such as significantly increased thermal

Table 8. Relative content in PEG involved the Cloisite®30B based nanocomposites (3 wt.-% in inorganics).

Code	PEG content	
	PEG ^{a)}	PEG ^{TGA b)}
	wt.-%	wt.-%
SC1N3B30	0.8	ND ^{c)}
SC5N3B30	4.4	4.7
SC10N3B30	8.5	10.7
SC20N3B30	16.2	16.8

^{a)} PEG content at start (see Table 7).

^{b)} As determined by TGA (from Figure 11a).

^{c)} Too low to be detected.

stability or higher degree of crystallinity compared to intercalated nanostructure at same clay loading. Moreover, intercalated nanocomposites have been successfully prepared starting directly from Cloisite[®]Na⁺, while melt blending this non-organomodified filler with preformed PLA only yields microcomposites. Interestingly enough, semi-exfoliated/semi-intercalated nanocomposites based on 3 wt.-% of Cloisite[®]30B and (plasticized) P(D,L-LA) have been successfully prepared by the redispersion in commercially available (plasticized) P(D,L-LA) of a highly filled masterbatch, itself prepared by in situ polymerization of L,L-lactide in presence of the nanofiller.

Finally, in situ polymerization of L,L-lactide conducted in presence of both dihydroxylated PEG 1000 and Cloisite[®]30B have been studied. P(L,L-LA-b-EG-b-L,L-LA) triblock copolymers have been synthesized in situ directly in presence of the organoclay. Whatever the weight ratio in PEG 1000 initially fixed, intensive clay platelets destructure has been achieved. The plasticizing effect of the PEG sequence, thus entrapped in the triblock copolymers have been highlighted by the significant T_g decrease of the nanocomposite, e.g., from 60 to 12 °C at 16.2 wt.-% content in PEG. Moreover, the thermal degradation of the resulting nanocomposites was dependent on the relative content in PEG blocks, and the thermal stability decreases as the polyether level increases within the triblock copolymer. In conclusion, this contribution shows the unique possibility to tune up the morphological and thermal properties of P(L,L-LA) layered silicate nanocomposites by adequately combining in situ catalytic polymerization “masterbatch” melt blending and matrix plasticization along with nanocomposition preparation.

Acknowledgements: M.-A. Paul thanks the F.R.I.A. (*Fonds pour la Recherche Industrielle et Agricole*) for her PhD grant. M. Alexandre is very grateful for the financial support from “*Région Wallonne*” and *European Community (FEDER, FSE)* in the frame of “*Pôle d'Excellence Materia Nova*.” LMPC thanks the *Belgian Federal Government Office of Science Policy (STC-PAI 5/3)*. C. Delcourt is much indebted to the “*Région Wallonne Programme WDU-TECMAVER*.”

- [1] [1a] S. Fischer, M. De Vlieger, T. Kock, L. Batenburg, H. Fischer, *Materialen* **2000**, *16*, 3; [1b] H. M. Park, W. K. Lee, C. Y. Park, W. J. Cho, C. S. Ha, *J. Mater. Sci.* **2003**, *38*, 909; [1c] J. P. Zheng, P. Li, Y. L. Ma, K. D. Yao, *J. Appl. Polym. Sci.* **2002**, *86*, 1189; [1d] J. P. Zheng, L. F. Xi, H. L. Zhang, K. D. Yao, *J. Mater. Sci. Lett.* **2003**, *22*, 1179; [1e] S.-R. Lee, H.-M. Park, L. Hyuntaek, T. Kang, X. Li, W.-J. Cho, C.-S. Ha, *Polymer* **2002**, *43*, 2495; [1f] S.-T. Lim, Y.-H. Hyun, H. J. Choi, M. S. Jhon, *Chem. Mater.* **2002**, *14*, 1839.
- [2] [2a] S. Sinha Ray, K. Yamada, M. Okamoto, K. Ueda, *Nano Lett.* **2002**, *2*, 1093; [2b] P. Maiti, K. Yamada, M. Okamoto, K. Ueda, K. Okamoto, *Chem. Mater.* **2002**, *14*, 4654.
- [3] S. S. Ray, P. Maiti, M. Okamoto, K. Yamada, K. Ueda, *Macromolecules* **2002**, *35*, 3104.
- [4] M.-A. Paul, M. Alexandre, Ph. Degée, C. Henrist, A. Rulmont, Ph. Dubois, *Polymer* **2003**, *44*, 443.
- [5] M. Alexandre, Ph. Dubois, *Mater. Sci. Eng.* **2000**, *28*, 1.
- [6] X. H. Liu, Q. J. Wu, L. A. Berglund, J. Q. Fan, Z. N. Qi, *Polymer* **2001**, *42*, 8235.
- [7] P. Reichert, J. Kressler, R. Thomann, R. Mühlaupt, G. Stöppelmann, *Acta Polym.* **1998**, *49*, 116.
- [8] X. Huang, W. J. Brittain, *Macromolecules* **2001**, *34*, 3255.
- [9] M. W. Weimer, H. Chen, E. P. Giannelis, D. Y. Sogah, *J. Am. Chem. Soc.* **1999**, *121*, 1615.
- [10] D. Kubies, N. Pantoustier, Ph. Dubois, A. Rulmont, R. Jérôme, *Macromolecules* **2002**, *35*, 3318.
- [11] B. Lepoittevin, N. Pantoustier, M. Devalckenaere, M. Alexandre, C. Calberg, R. Jérôme, Ph. Dubois, *Macromolecules* **2002**, *35*, 8385.
- [12] B. Lepoittevin, N. Pantoustier, M. Alexandre, D. Kubies, C. Calberg, R. Jérôme, Ph. Dubois, *J. Mater. Chem.* **2002**, *12*, 3528.
- [13] M.-A. Paul, M. Alexandre, Ph. Degée, C. Calberg, R. Jérôme, Ph. Dubois, *Macromol. Rapid Commun.* **2003**, *24*, 561.
- [14] Ph. Degée, Ph. Dubois, R. Jérôme, *Macromol. Chem. Phys.* **1997**, *198*, 1985.
- [15] Ph. Dubois, C. Jacobs, R. Jérôme, Ph. Teyssié, *Macromolecules* **1991**, *24*, 2266.
- [16] A. Kowalski, A. Duda, S. Penczek, *Macromolecules* **2000**, *33*, 7359.
- [17] I. Barakat, Ph. Dubois, R. Jérôme, Ph. Teyssié, *J. Polym. Sci., Part A: Polym. Chem.* **1993**, *31*, 505.
- [18] B. Lepoittevin, N. Pantoustier, M. Alexandre, C. Calberg, R. Jérôme, Ph. Dubois, *Macromol. Symp.* **2002**, *183*, 95.
- [19] M. Pluta, A. Galeski, M. Alexandre, M.-A. Paul, Ph. Dubois, *J. Appl. Polym. Sci.* **2002**, *86*, 1497.
- [20] A. Gaudel-Siri, P. Brocorens, D. Siri, F. Gardebien, J.-L. Brédas, R. Lazzaroni, *Langmuir* **2003**, *19*, 8287.
- [21] B. Lepoittevin, N. Pantoustier, M. Devalckenaere, M. Alexandre, C. Calberg, R. Jérôme, C. Henrist, A. Rulmont, Ph. Dubois, *Polymer* **2003**, *44*, 2033.
- [22] X. Zheng, C. A. Wilkie, *Polym. Degrad. Stab.* **2003**, *82*, 441.
- [23] Y. Hu, M. Rogunova, V. Topolkaev, A. Hiltner, E. Baer, *Polymer* **2003**, *44*, 5701.
- [24] Y. Hu, Y. S. Hu, V. Topolkaev, A. Hiltner, E. Baer, *Polymer* **2003**, *44*, 5711.
- [25] D. Cam, M. Marucci, *Polymer* **1997**, *38*, 1879.